

# Lateral Packing of the Pancreatic Lipase Cofactor, Colipase, with Phosphatidylcholine and Substrates<sup>†</sup>

Maureen M. Momsen, Mohammed Dahim, and Howard L. Brockman\*

*The Hormel Institute, University of Minnesota, Austin, Minnesota 55912*

*Received February 19, 1997; Revised Manuscript Received June 13, 1997<sup>®</sup>*

**ABSTRACT:** The interaction of the pancreatic lipase cofactor colipase with a diacylphosphatidylcholine, acylglycerols, and free fatty acid was investigated by monitoring its adsorption to monomolecular lipid films. Surface pressure and colipase surface concentration were measured as a function of the initial lipid concentration and composition. Colipase adsorbs to a level of 28–30 pmol/cm<sup>2</sup> to form a close-packed monolayer of protein and interacts strongly with all lipids when the lipid chain:colipase ratio is ≤3. Consideration of the size difference between the protein and acyl groups suggests that in this regime the lipid is occupying the voids between tightly packed protein molecules. At lipid chain:colipase ratios >3, the triacylglycerol is excluded from the monolayer phase. Phosphatidylcholine, diacylglycerols, and free fatty acid remain in the monolayer phase up to ≤25 lipid chain:colipase ratios. Geometrically over this range of compositions, the colipase molecules should be separated by up to 0–2 acyl chains. At higher lipid chain:colipase ratios, diacylglycerols are likely excluded from the monolayer phase. Anomalous behavior is observed with the fatty acid which at lipid chain:colipase ratios >25 induces higher levels of colipase adsorption than at lower ratios. This suggests the formation of a novel structure involving fatty acid and/or colipase. Phosphatidylcholine also remains in the interface at lipid chain:colipase ratios >3 but shows little additional interaction with colipase. However, fluorescence microscopy suggests that the phosphatidylcholine and colipase are miscible in the interface. The specificity demonstrated in this study suggests that colipase may regulate the type of surfaces to which colipase and, hence, lipase bind and may control the species distribution of substrate to which bound lipase is exposed.

Ingested dietary triacylglycerols are emulsified and partially hydrolyzed to 1,2-diacylglycerols and fatty acids in the stomach (1). The emulsion then passes to the duodenum where bile is added and the acylglycerols are attacked by secreted pancreatic triacylglycerol lipase and carboxylester lipase (2–5). The addition of biliary bile salts and phospholipids aids in the emulsification of the acylglycerols and generates a micellar phase for the transport of fatty acids and 2-monoacylglycerols to the intestinal villus membrane (2). However, studies of lipolysis *in vitro* have shown that bile salts and phospholipids inhibit pancreatic lipase, primarily by preventing its adsorption to the substrate-containing surface of the emulsion particles (3). Pancreatic lipase-catalyzed lipolysis proceeds under physiological conditions because the pancreas also secretes a 10 kDa cofactor protein which enables lipolysis to occur in a bile salt- and phospholipid-rich milieu (5–7).

Soon after the discovery of the colipase, it was recognized that it is secreted as a procoprotein, named procolipase, which is converted to colipase by the tryptic cleavage of an N-terminal pentapeptide (6, 8). Chymotryptic cleavage of two residues near the C-terminus of procolipase has also been observed during its purification from pancreas (9), but no functional or structural significance of this proteolysis has been documented (10). The conversion of procolipase to

colipase was observed to enhance its activity by reducing the delays or “lag times” observed before the onset of lipid hydrolysis after pancreatic lipase is added to a phospholipid–substrate emulsion (8, 11). This has been attributed to colipase having a higher affinity for phospholipid-rich interfaces than procolipase (11). Subsequently, it was observed that the N-terminal pentapeptide, enterostatin, which was released when procolipase was converted to colipase could be absorbed and function as a satiety factor (12, 13). Additionally, new studies comparing procolipase and colipase function at physiological pH, as opposed to the high pH used previously, showed no significant difference between the two forms of the cofactor (14). This led to the proposal that at physiological pH the conversion of procolipase to colipase is of no functional significance with respect to the immediate function of colipase in lipid digestion (14).

Studies of colipase function have also revealed effects of free fatty acids on its ability to stimulate lipolysis in the presence of phospholipids and bile salts. These led to the suggestions that the functional catalytic unit was a lipase–colipase–fatty acid complex (15) and that clusters of the calcium salts of fatty acids enhanced colipase adsorption to phospholipid-rich interfaces (16). In addition, the partial hydrolysis of triacylglycerols, such as occurs in the stomach, eliminates lag times following lipase addition (15, 17). However, the precise mechanism(s) by which fatty acids and partial glycerides regulate colipase function remained unknown. To better understand how the various components of this system function, this laboratory has undertaken a systematic investigation of lipid–colipase–lipase interactions

<sup>†</sup> This work was supported by USPHS Grant HL49180 and by the Hormel Foundation.

\* Address correspondence to this author at The Hormel Institute, University of Minnesota, 801 16th Ave. NE, Austin, MN 55912. Telephone: (507)437-9620. Fax: (507)437-9696 or -9606. E-mail: hlbroc@maroon.tc.umn.edu.

<sup>®</sup> Abstract published in *Advance ACS Abstracts*, August 1, 1997.

in monomolecular films comprised of diacylphosphatidylcholine, not a lipase substrate, and acylglycerol substrates at a physiologically relevant pH. Initially, it was demonstrated that the initiation of lipase action toward phosphatidylcholine—substrate mixed monolayers in the absence of colipase requires a critical mole fraction of substrate to be present (18). Additionally, separate physical measurements of lipid miscibility confirmed that the lipids themselves did not phase-separate at the critical composition (19).

As the first step to understanding how lipase cofactor proteins regulate lipolysis, procolipase adsorption to phosphatidylcholine—substrate mixed monolayers was characterized in the absence of lipase. This study showed that there was a preferential interaction of procolipase with model lipase substrates, i.e., 1,3-diacylglycerol (1,3-DO)<sup>1</sup> or 13,16-*cis,cis*-docosadienoic acid (DA), compared with 1-stearoyl-2-oleoyl-*sn*-glycero-3-phosphocholine (SOPC) (20). Next, to test the functional significance of the conversion of procolipase and colipase, competitive adsorption studies were carried out (21). These showed clearly that, in the presence of lipids, colipase quantitatively displaced procolipase from monolayers, suggesting possible differences in the way the two forms of the cofactor interact with lipids. Because of this, studies of colipase adsorption to SOPC—substrate monolayers were undertaken. As reported herein, the results show that even though it is more surface-active than procolipase, colipase also interacts preferentially with substrate as compared to SOPC. More importantly, improvements in the assay for measuring adsorption of colipase to monolayers reveal important insights concerning the packing of lipid and cofactor as a function of their relative abundance in the interface.

## MATERIALS AND METHODS

1,3-Dioleoylglycerol (1,3-DO) and 13,16-*cis,cis*-docosadienoic acid (DA) were from NuChek Prep, Inc. (Elysian, MN), 1-stearoyl-2-oleoyl-*sn*-glycero-3-phosphocholine (SOPC) from Avanti Polar Lipids (Alabaster, AL), 1,2-dioleoylglycerol (1,2-DO) and 1,2-dioleoyl-3-stearoyl-*rac*-glycerol (OOS) from Sigma (St. Louis, MO), and 1-palmitoyl-2-(4,4-difluoro-5,7-dimethyl-4-bora-3a,4a-diaza-s-indacene-3-dodecyl)-*sn*-glycero-3-phosphocholine (BODIPY PC) from Molecular Probes (Eugene, OR). All lipids were dissolved in hexane/ethanol (95:5). Solvents, buffer, and lipid solutions were prepared as described (22). Water for preparation of buffer was purified by reverse osmosis, activated charcoal adsorption, and mixed-bed deionization and then passed through a Milli-Q UV Plus System (Millipore Corp., Bedford, MA) equipped with a 0.22  $\mu\text{m}$  Millipak 40 membrane.

The preparation of colipase and its conversion to [<sup>14</sup>C]-colipase have been described previously (21). The specific activity of the purified colipase was 41 000 units/mg. The radiolabeled colipase had a specific activity of 39 000 units/mg and a specific radioactivity of 9.76  $\mu\text{Ci/mol}$ , corresponding to a labeling efficiency of  $\sim 30\%$ . For fluorescence microscopy lipids and colipase were dissolved in chloroform/

methanol/water (5:5:1) (M. Dahim and H. L. Brockman, submitted for publication).

The methodology and instrumentation for spreading lipid monolayers, monitoring surface pressure changes, and quantifying [<sup>14</sup>C]colipase adsorption to lipid monolayers have been described (21, 23). Briefly, adsorption of [<sup>14</sup>C]colipase to lipid monolayers was measured using a circular Teflon trough (19.5 mL, 20.4 cm<sup>2</sup>) filled with 10 mM phosphate, pH 6.6, 0.1 M NaCl, and 0.01% NaN<sub>3</sub> at 24 °C. Lipid was spread to the desired surface concentration, and the monolayer was allowed to stabilize for 5–10 min. Stirring of the aqueous phase at 50 rpm was begun, and 5  $\mu\text{Ci}$  of [<sup>32</sup>P]-phosphate and a saturating amount of [<sup>14</sup>C]colipase (240 nM in the trough) were sequentially injected under the lipid monolayer. After 30 min, the monolayer was collected using hydrophobic paper. The paper was cut into pieces and placed into a scintillation vial, and [<sup>14</sup>C]colipase and [<sup>32</sup>P]phosphate were determined by liquid scintillation counting. An aliquot of subphase was also collected for determination of both [<sup>14</sup>C]colipase and [<sup>32</sup>P]phosphate. An efficiency of monolayer collection of 84% was used, based on prior calibration. The levels of [<sup>32</sup>P]phosphate in the subphase and the collected monolayer were used to correct the measured adsorption of [<sup>14</sup>C]colipase for subphase carryover on the hydrophobic paper. For 68 experiments with a variety of lipid compositions and surface concentrations, the correction was small, exhibiting a range of 0.25–0.90 pmol/cm<sup>2</sup> with an average value of 0.54 pmol/cm<sup>2</sup>. In contrast, values for net colipase adsorption ranged from 1 to 30 pmol/cm<sup>2</sup>.

Fluorescence microscopy of SOPC/BODIPY PC/colipase monolayers was performed using a Kibron  $\mu$ Trough computer-controlled film balance (Helsinki, Finland). Trough area was controlled and data were collected and analyzed by FilmWare, dedicated software provided by Kibron. The balance rested on the stage of a Zeiss IM-35 inverted microscope equipped with a 20 $\times$  Nikon Model 85052 (0.4 NA) objective. Excitation was at 450–490 nm, and fluorescence was observed either at  $\geq 520$  nm (green + red wavelengths) or at  $\geq 590$  nm (red wavelengths) (24).

## RESULTS

In an earlier study (20), the preferential interaction of procolipase with pancreatic lipase substrates, as opposed to phosphatidylcholine, was indicated by anomalous increases in surface pressure when the protein was injected beneath substrate-rich monomolecular lipid films. To determine if the same preference is exhibited by colipase and to what extent it occurs, studies similar to those reported earlier were carried out with colipase. Specifically, a saturating amount of [<sup>14</sup>C]colipase (21) was injected under monolayers of SOPC, DA, 1,3-DO, 1,2-DO, OOS, and selected mixtures at various initial surface pressures. For any lipid composition, the value of the initial surface pressure,  $\pi_i$ , is a direct function of the surface concentration of lipid. The substitution of [<sup>14</sup>C]colipase for native colipase and procolipase used in earlier studies was made to eliminate the scatter in the results caused by the catalytic assay used to quantitate the cofactor after its recovery from the lipid–water interface. Because [<sup>14</sup>C]colipase and native colipase compete equally for interfacial occupancy in both the presence and the absence of lipid (21), this substitution has no effect on the measured adsorption of cofactor. Following the injection of [<sup>14</sup>C]-

<sup>1</sup> Abbreviations: 1,3-DO, 1,3-dioleoylglycerol; DA, 13,16-*cis,cis*-docosadienoic acid; SOPC, 1-stearoyl-2-oleoyl-*sn*-glycero-3-phosphocholine; 1,2-DO, 1,2-dioleoylglycerol; OOS, 1,2-dioleoyl-3-stearoyl-*rac*-glycerol; BODIPY PC, 1-palmitoyl-2-(4,4-difluoro-5,7-dimethyl-4-bora-3a,4a-diaza-s-indacene-3-dodecyl)-*sn*-glycero-3-phosphocholine.

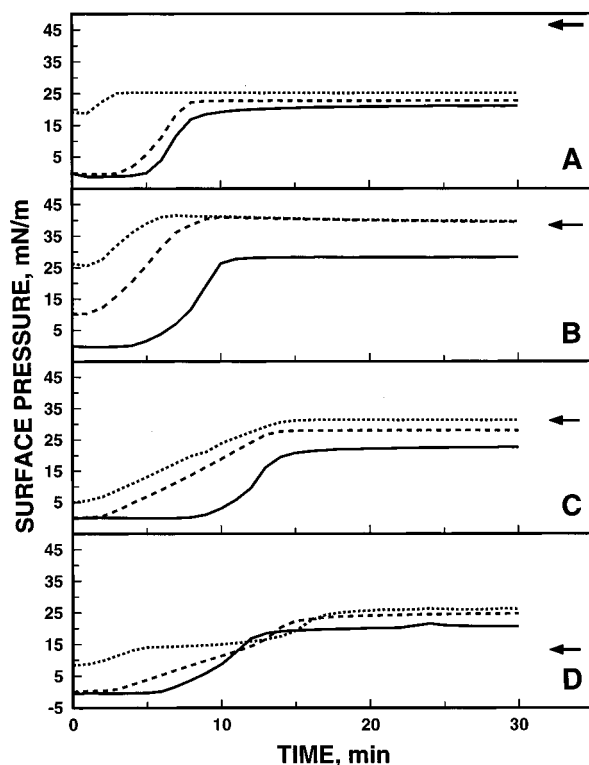


FIGURE 1: Time-dependent surface pressure changes induced by injection of colipase beneath lipid monolayers. Arrows indicate the collapse surface pressure of the lipid monolayer alone. Colipase (240 nM) was injected under monolayers of (A) SOPC, (B) DA, (C) 1,2-DO or (D) OOS at initial lipid concentrations of (A) 34 (—), 104 (---), and 240 (···); (B) 177 (—), 458 (---), and 545 (···); (C) 53 (—), 173 (---), and 221 (···); and (D) 63 (—), 105 (---), and 164 (···) pmol/cm<sup>2</sup>.

colipase to a final concentration of 240  $\mu$ M in the stirred aqueous subphase, the surface pressure of the monolayer was monitored for 30 min. Representative time courses obtained with the one-component monolayers, shown in Figure 1, indicate that surface pressures became essentially constant during the exposure to [<sup>14</sup>C]colipase. Note that for each experiment the final and, generally, highest surface pressure reached,  $\pi_f$ , increases directly with the initial surface pressure,  $\pi_i$ , and approaches a limit. The surface tension at an interface between two phases such as argon and water describes the interfacial free energy per unit area. The surface pressure is the change in that free energy induced by lipids, proteins, or other constituents added to the interface and is typically expressed as mN/m (= ergs/cm<sup>2</sup>). As defined, an increase in surface pressure is numerically equal to the decrease in the surface tension, i.e., the lowering of interfacial free energy. Hence, the size of the [<sup>14</sup>C]colipase-induced surface pressure increases at constant surface area indicates the extent to which [<sup>14</sup>C]colipase adsorption and interaction with lipids stabilize the interface. For each lipid species, as well as their mixtures (Table 1), the highest value of  $\pi_f$  exceeded that of  $18.4 \pm 1.9$  mN/m observed with [<sup>14</sup>C]colipase in the absence of lipid (21). This indicates that energetically favorable interactions between the lipids and [<sup>14</sup>C]colipase accompany adsorption. If that were not the case, [<sup>14</sup>C]colipase adsorption would cease if lipids were spread to an initial surface pressure,  $\pi_i$ ,  $> 18.4$  mN/m, ignoring the entropic contribution of ideal colipase–lipid mixing in the interface. Rather, the maximum  $\pi_f$  for each lipid species  $\gg 18.4$  mN/m (Table 1), with the exception

of SOPC (Figure 1A), equals or exceeds the collapse surface pressure of the lipids alone (Table 1 and Figure 1, arrows). These values of  $\pi_f$  and the observation that the highest observed  $\pi_f$  for SOPC is less than or equal to the collapse pressures of DA, 1,3-DO, and 1,2-DO alone (Table 1) indicate that [<sup>14</sup>C]colipase interacts more strongly with these lipase substrates than with SOPC upon its adsorption to the lipid monolayer. For SOPC and OOS, the highest observed  $\pi_f$  values are approximately equal. For the various mixtures tested (Table 1), values of  $\pi_f$  intermediate between or exceeding those for the individual species were obtained. This indicates that preferential interactions of [<sup>14</sup>C]colipase with substrates also occur in mixed lipid films.

Inspection of Figure 1 shows that as  $\pi_i$  is increased above 1 mN/m, its difference from  $\pi_f$ , the value at 30 min for each curve, decreases. In general, for surfactant adsorption to monolayers at a fixed composition, linear extrapolation to zero of the change in surface pressure as a function of increasing initial surface pressure is used to determine the highest initial pressure at which a change occurs (e.g., ref 20 and references cited therein). This is exemplified in Figure 2 which shows changes in surface pressure which accompany [<sup>14</sup>C]colipase adsorption to monolayers of DA, 1,2-DO, and SOPC as a function of  $\pi_i$ . For each data set, the changes in surface pressure reach a maximum at  $\pi_i$  values associated with the lipid monolayer being in the liquid-expanded state, i.e., 0–1 mN/m. At higher  $\pi_i$ , the changes decrease toward zero in the expected linear manner. Extrapolation of the linear portion of each data set to the abscissa by least-squares fitting yields the initial surface pressure at which no change in surface pressure would be observed. This extrapolated limit is designated  $\pi_{i|\Delta\pi=0}$ , and the values obtained for all lipid mixtures studied are summarized in Table 1. Also given in the table are the values of the lowest initial surface pressure on which the extrapolation was based, designated low  $\pi_i$ . The value of  $\pi_{i|\Delta\pi=0}$  relative to the maximum surface pressure observed for the adsorption of [<sup>14</sup>C]colipase alone, 18.4 mN/m, is a measure of the strength of the lipid–protein interaction. Note from the values of low  $\pi_i$  in the table that at higher mole fractions of substrate in mixtures with SOPC the relative lack of linearity of the plots necessitated fitting only data points obtained at higher values of  $\pi_i$ . Table 1 shows that the values of  $\pi_{i|\Delta\pi=0}$  obtained for films containing a high proportion of substrate can, like the maximum  $\pi_f$ , exceed both the collapse pressure of the lipid monolayer in the absence of [<sup>14</sup>C]colipase as well as the maximum surface pressure reached for the adsorption of [<sup>14</sup>C]colipase in the absence of lipid. This indicates a stabilizing interaction between the substrate-rich monolayers and [<sup>14</sup>C]colipase which lowers the interfacial free energy more than does the presence of lipid alone. That values of  $\pi_{i|\Delta\pi=0}$  in Table 1 often exceed the maximum  $\pi_f$  reflects the fact that  $\pi_{i|\Delta\pi=0}$  is an extrapolated quantity whereas maximum  $\pi_f$  is measured experimentally using monolayers for which  $\pi_i$  cannot exceed the collapse surface pressure of the monolayer.

In an earlier study of procolipase adsorption to lipid monolayers (20), its surface concentration exhibited an apparently inverse linear relationship to the surface concentration of lipid in the monolayer,  $\Gamma_L$ , at each lipid composition. This behavior suggested that procolipase and lipid compete for occupancy of the interface in the same plane and that procolipase adsorption is limited by a minimal

Table 1: Surface Pressure ( $\pi$ , mN/m) and Area Data for Colipase Adsorption to Lipid Monolayers

monolayer		surface pressure (mN/m)				molecular areas ( $\text{\AA}^2$ )	
lipids	composition	collapse $\pi^a$	max $\pi_f^b$	low $\pi_i^c$	$\pi_i _{\Delta\pi=0}^d$	lipid	colipase
DA/SOPC	0/1	46.6	27.7	4	26.0	74.8	498.3
	0.196/0.804	46.6	27.0	3	29.1	59.6	502.5
	0.401/0.599	45.9	34.6	3	36.0	53.9	494.5
	0.500/0.500	45.7	37.7	3	38.1	50.8	467.1
	0.607/0.397	45.1	38.8	3	43.1	51.1	442.5
	0.798/0.202	42.1	42.9	11	46.4	37.4	469.1
1,3-DO/SOPC	1/0	38.4	41.9	11	41.2	22.1	484.8
	0.210/0.790	47.5	34.9	10	31.8	66.8	486.0
	0.334/0.666	41.3	38.2	7	34.0	60.8	510.8
	0.398/0.602	37.3	36.3	9	40.4	54.5	522.3
	0.605/0.395	31.6	36.3	18	37.2	54.2	475.5
	0.799/0.201	29.1	34.8	14	34.9	46.2	464.8
1,3-DO/DA/SOPC	1/0	27.7	34.5	12	34.8	33.8	508.6
	0.124/0.375/0.501	46.1	37.0	15	43.1	49.8	480.7
	0.252/0.247/0.501	41.6	42.1	10	51.9	44.4	513.5
1,3-DO/DA	0.372/0.125/0.503	38.7	35.3	15	36.8	38.4	508.4
	0.244/0.756	34.4	41.2	25	41.2	17.2	532.9
	0.497/0.503	31.7	40.0	20	39.8	22.9	515.4
1,2-DO	0.754/0.246	29.5	37.4	18	37.6	32.4	512.5
	1.000	31.5	36.8	5	38.4	38.5	516.2
OOS	1.000	13.2	27.0	1	27.2		

<sup>a</sup> Measured surface pressure at monolayer collapse in the absence of colipase. <sup>b</sup> Highest surface pressure reached following addition of 240 nM colipase under lipid monolayers. <sup>c</sup> Lowest initial surface pressure used in the linear extrapolation to obtain  $\pi_i|_{\Delta\pi=0}$  for each set of lipid monolayers.

<sup>d</sup> Molecular areas for lipid and colipase determined as the reciprocals of the abscissa and the ordinate, respectively, of lines of the type shown in Figures 3–6.

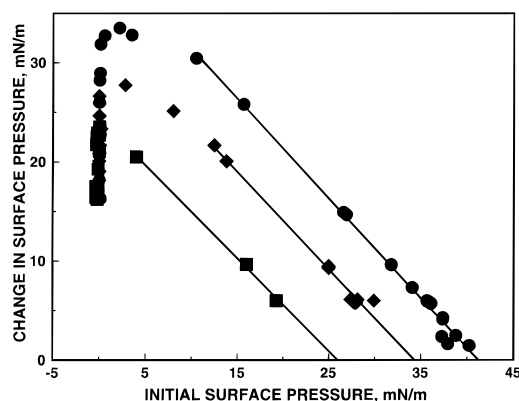


FIGURE 2: Equilibrium surface pressure changes induced by injection of colipase beneath lipid monolayers at various initial surface pressures. Lipids: (●) DA, (◆) 1,2-DO, (■) SOPC.

molecular area to which the lipid can be compressed. Thermodynamically, adsorption equilibrium occurs when the energy gained by adsorption of each procolipase molecule equals the work required to compress the lipids to create a site for it to adsorb. Thus, the apparent geometric nature of this model implies that the energy required to compress the lipid below its minimal area increases discontinuously at the minimal lipid area. The range of  $\Gamma_L$  over which this competitive behavior was tested and observed was limited to  $\Gamma_L$  values for which the collapse surface pressure of the lipid monolayer prior to protein addition was not exceeded. However, *in vivo*, colipase functions on lipid emulsions in which a bulk substrate phase exists in addition to the interfacial phase. Such emulsions can be modeled by using a monolayer compressed beyond its collapse pressure. For this reason, in the present study, lipid concentrations which exceeded the value of  $\Gamma_L$  at monolayer collapse were used in some cases.

To determine if [ $^{14}\text{C}$ ]colipase adsorption exhibited behavior similar to that of procolipase, values of the surface concentration of colipase in the monolayer,  $\Gamma_C$ , determined from

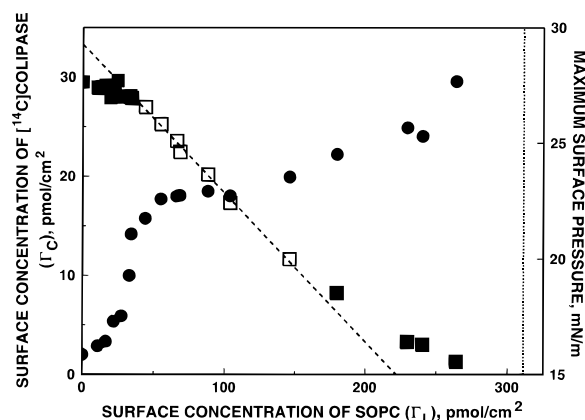


FIGURE 3: Dependence of [ $^{14}\text{C}$ ]colipase adsorption and accompanying surface pressure changes on SOPC concentration. (■, □) Surface concentration of [ $^{14}\text{C}$ ]colipase,  $\Gamma_C$ ; (●) final surface pressure,  $\pi_f$ . The open squares (□) indicate the values used to fit the dashed line (- - -). The vertical dotted line (···) indicates the highest value of  $\Gamma_L$  for which the lipid alone exhibited monolayer behavior.

monolayers collected following experiments of the type shown in Figure 1, were plotted as a function of  $\Gamma_L$ . These are shown for SOPC, DA, 1,3-DO, 1,2-DO, and OOS in Figures 3–7. Also shown for each measurement of  $\Gamma_L$  is the corresponding value of  $\pi_f$ . In each figure, the vertical dotted line indicates the lipid concentration at which the monolayer collapses in the absence of [ $^{14}\text{C}$ ]colipase. It should be noted that the term surface concentration as applied to the axes in Figures 3–7 refers to the total amount of lipid added to or colipase adsorbed into the interface divided by the area of the trough. As will be described in detail below, under some conditions part or all of the interfacial components may not be present as a simple monomolecular layer, but may exist as a multilayer or nonaqueous bulk phases.

It is obvious from inspection of Figures 3–7 that the relationship between [ $^{14}\text{C}$ ]colipase concentration and lipid concentration is not simply linear, even if only the region

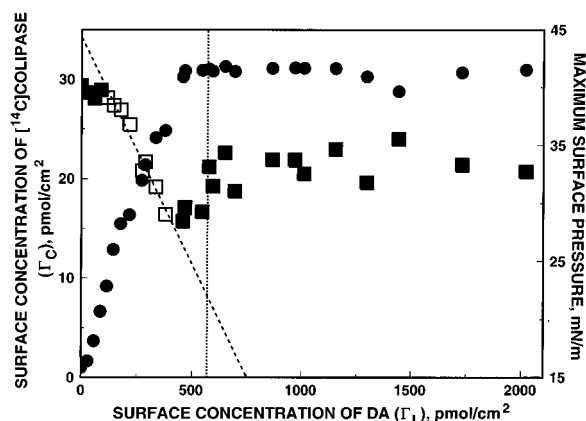


FIGURE 4: Dependence of  $[^{14}\text{C}]$ colipase adsorption on DA concentration. Legend as in Figure 3.

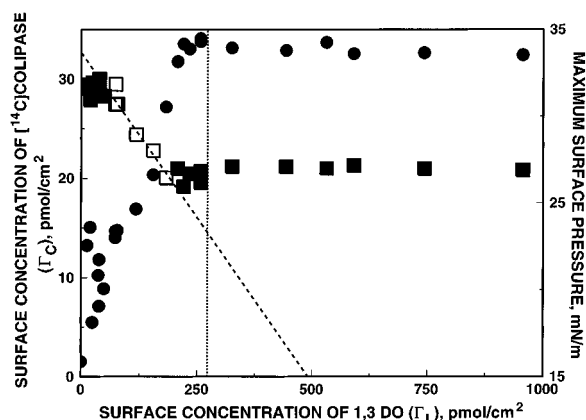


FIGURE 5: Dependence of  $[^{14}\text{C}]$ colipase adsorption on 1,3-DO concentration. Legend as in Figure 3.

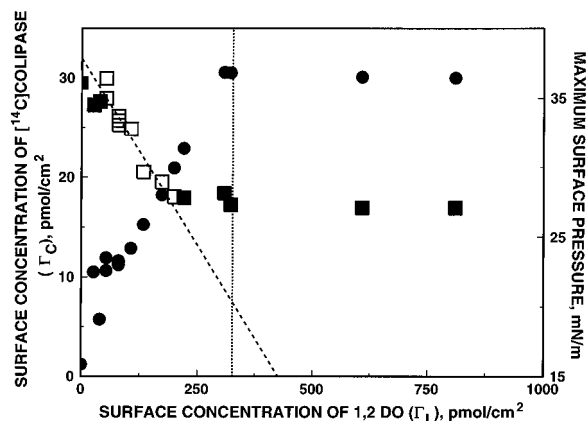


FIGURE 6: Dependence of  $[^{14}\text{C}]$ colipase adsorption on 1,2-DO concentration. Legend as in Figure 3.

of initial monolayer lipid coverage, *i.e.*, to the left of the dotted line, is considered. Instead, several types of behavior can be observed. For all lipids at lower  $\Gamma_L$ , values of  $\Gamma_C$  decline little as  $\Gamma_L$  is increased. For OOS (Figure 7), this behavior continues over the entire monolayer region, the range over which data were collected for this lipid. For the other species (Figures 3–6), the region of invariance is followed by an apparently linear region (dashed line) in which  $\Gamma_C$  decreases as  $\Gamma_L$  is further increased. Beyond this linear range,  $[^{14}\text{C}]$ colipase adsorption becomes more lipid species specific. For SOPC, adsorption of  $[^{14}\text{C}]$ colipase decreases continuously with increasing  $\Gamma_L$  and appears to be approaching a limit of zero at the line indicating the monolayer limit (Figure 3). For  $[^{14}\text{C}]$ colipase adsorption to

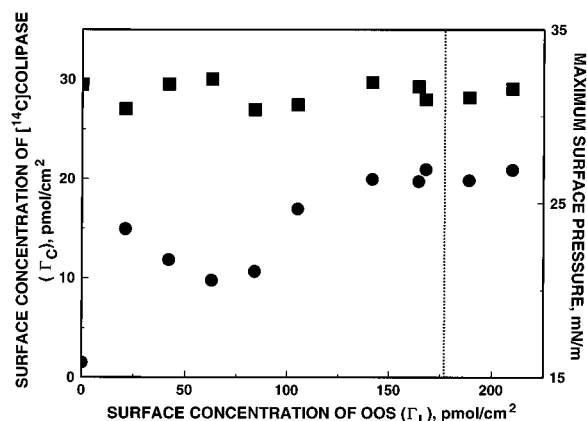


FIGURE 7: Dependence of  $[^{14}\text{C}]$ colipase adsorption on OOS concentration. Legend as in Figure 3.

the lipase substrates 1,3-DO and 1,2-DO (Figures 5 and 6),  $\Gamma_C$  abruptly becomes independent of  $\Gamma_L$  at approximately 21 and 17 pmol/cm<sup>2</sup> of  $[^{14}\text{C}]$ colipase, respectively. For those lipids, the highest value of  $\Gamma_L$  used was approximately double for 1,2-DO and 3.5 times the monolayer coverage for 1,3-DO. Yet a different adsorption behavior following the region of linear decline of  $\Gamma_C$  with  $\Gamma_L$  is exhibited with DA (Figure 4). As  $\Gamma_L$  is increased from its value at the end of the linear region toward the monolayer limit,  $\Gamma_C$  increases from 16 pmol/cm<sup>2</sup> to a value of about 22 pmol/cm<sup>2</sup>. With a further increase in  $\Gamma_L$ ,  $\Gamma_C$  remained essentially constant to the study limit of 3.5 times the initial monolayer coverage.

The values of  $\pi_f$  in the experiments described above also depend on  $\Gamma_L$ . Despite the fact that  $\Gamma_C$  is independent of OOS concentration,  $\pi_f$  increases from 16 mN/m to 23.5 mN/m as  $\Gamma_L$  increases from 20 nmol/cm<sup>2</sup>, decreases to a minimum of 20.5 mN/m at a  $\Gamma_L$  of 60–70 nmol/cm<sup>2</sup>, and reaches a maximum of 26.5 mN/m at a  $\Gamma_L$  in the vicinity of 130 nmol/cm<sup>2</sup> (Figure 7). For the remainder of the lipid species,  $\pi_f$  increases rapidly at low  $\Gamma_L$ , *i.e.*, where  $\Gamma_C$  is approximately constant. The rate of increase of  $\pi_f$  with increasing  $\Gamma_L$  slows as the region of linear  $\Gamma_C$  vs  $\Gamma_L$  is entered. For  $[^{14}\text{C}]$ colipase adsorption to SOPC, values of  $\pi_f$  are essentially constant in the linear region, after which they slowly increase to a maximum of 28 mN/m as the limit of  $[^{14}\text{C}]$ colipase adsorption is approached (Figure 3). For  $[^{14}\text{C}]$ colipase adsorption to 1,2-DO, 1,3-DO, and DA, values of  $\pi_f$  reach their respective maximums (Table 1) at or before the value of  $\Gamma_L$  representing the monolayer limit (Figures 4–6). Above the monolayer limit, they remain constant.

The adsorption of  $[^{14}\text{C}]$ colipase to a number of lipid mixtures was also studied (Table 1). These studies, exemplified in Figures 8–10, were generally more limited with respect to the number of  $\Gamma_L$  values tested. Figure 8 is a composite of  $\Gamma_C$  vs  $\Gamma_L$  isotherms obtained with mixtures of 1,3-DO and DA. Note that  $[^{14}\text{C}]$ colipase adsorption to 3:1 and 1:1 mixtures of 1,3-DO/DA shows a constant  $\Gamma_C$  value at higher values of  $\Gamma_L$ , as did pure 1,3-DO. In contrast, the 1:3 mixture shows a minimum value of  $\Gamma_C$  similar to that exhibited by DA alone. Equimolar mixtures of SOPC and DA were examined as a function of pH between 5.5 and 8.5 (Figure 9). This pH range encompasses the highest and lowest values observed in duodenal aspirates during digestion of a test meal (25). These mixtures show identical behavior at all pH values. That behavior is similar to that exhibited by SOPC alone (Figure 3) in that  $\Gamma_C$  decreases monotonically

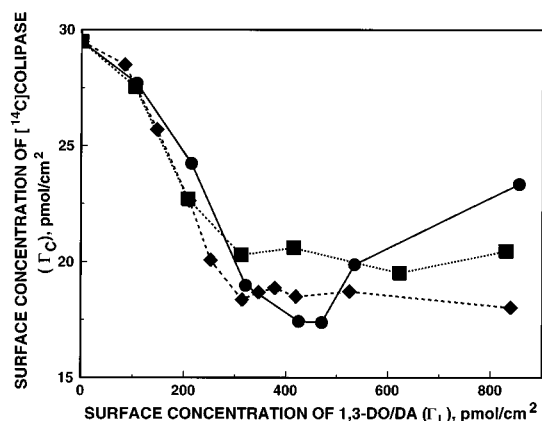


FIGURE 8: Dependence of  $[^{14}\text{C}]$ colipase adsorption on surface concentration of 1,3-DO/DA mixtures. DO:DA ratios of 3:1 (■), 1:1 (◆), and 1:3 (●).

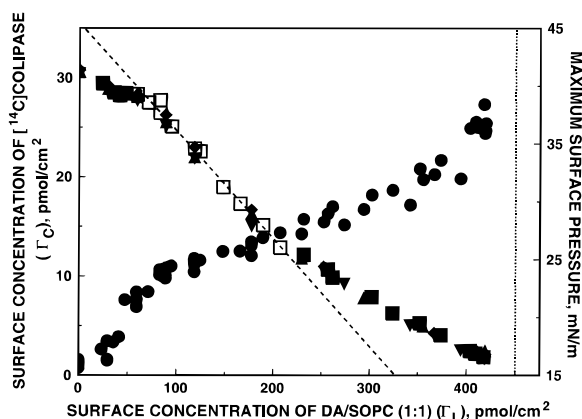


FIGURE 9: Effect of pH on  $[^{14}\text{C}]$ colipase adsorption to SOPC/DA (1:1) monolayers. Maximum surface pressure attained at all pH values (●) and surface concentrations of  $[^{14}\text{C}]$ colipase at (▲) pH 5.5, (■, □) pH 6.6, (◆) pH 7.5, and (▼) pH 8.5. The open squares (□) indicate the values used to fit the dashed line (---).

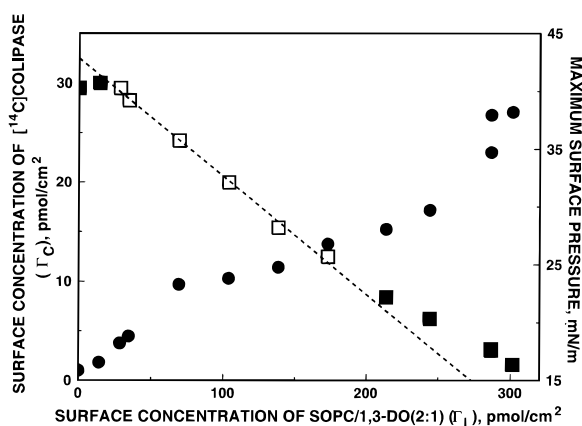


FIGURE 10: Dependence of  $[^{14}\text{C}]$ colipase adsorption on concentration of SOPC/1,3-DO mixtures (2:1). Legend as in Figure 3.

with increasing  $\Gamma_L$  following the linear segment of the isotherm. As exemplified in Figure 10,  $[^{14}\text{C}]$ colipase adsorption to a 2:1 mixture of SOPC and 1,3-DO also showed the absence of a lower limit of  $\Gamma_C$ , as did 3-component mixtures of SOPC, 1,3-DO, and DA (not shown). Comparison of Figures 9 and 10 with Figures 3–5 shows that the values of  $\pi_f$  and  $\Gamma_C$  are intermediate between those obtained with SOPC and substrate alone. In general, the behavior of these and other mixtures with respect to  $\pi_f$  and  $\Gamma_C$  varied continuously between the extremes observed; i.e., there was

no indication of any stoichiometric relationships between the lipids regulating  $[^{14}\text{C}]$ colipase adsorption.

The independence of the surface pressure of SOPC– $[^{14}\text{C}]$ colipase mixtures over a range of compositions suggested that they might be immiscible. To test this, mixed monolayers of SOPC/BODIPY PC/colipase (90:5:5) were prepared and examined between 1 and 25 mN/m by fluorescence microscopy. Under all conditions, only homogeneous fluorescence was observed. The absence of any discernible domain formation or fluorescence in homogeneities is consistent with the miscibility of the compounds.

## DISCUSSION

The ability of colipase to function in pancreatic lipase-catalyzed lipid hydrolysis depends on its ability to interact with the lipids which comprise the substrate-containing lipid–water interface. We showed earlier that such interaction exhibits specificity for procolipase adsorption to interfaces containing pancreatic lipase substrates as compared to diacylphosphatidylcholine (20). The present study tested the ability of  $[^{14}\text{C}]$ colipase to adsorb to those and additional interfaces. The use of  $[^{14}\text{C}]$ colipase in place of unlabeled colipase facilitated and improved the measurements. Importantly, it has been shown that in the presence and absence of both SOPC and DA the adsorption of  $[^{14}\text{C}]$ colipase accurately reflects that of colipase (21). The results of the present study show that  $[^{14}\text{C}]$ colipase adsorption to interfaces exhibits the same specificity with respect to SOPC vs 1,3-DO and DA, the substrates tested earlier. The generally higher values of  $\pi_i$  obtained for  $[^{14}\text{C}]$ colipase adsorption to these lipids and their mixtures (Table 1) as compared to procolipase (20) are consistent with the ability of  $[^{14}\text{C}]$ colipase to quantitatively displace procolipase from interfaces in the presence, but not the absence, of lipid (21).

Also tested in this study were 1,2-DO, a model physiological substrate of pancreatic lipase (17), and OOS, a model triacylglycerol. The interaction of  $[^{14}\text{C}]$ colipase with 1,2-DO was similar to that with 1,3-DO but apparently stronger. Both the value of  $\pi_i|_{\Delta\pi=0}$  as well as the maximum value of  $\pi_f$  (Table 1) were higher for  $[^{14}\text{C}]$ colipase adsorption to 1,2-DO than for 1,3-DO. This may simply reflect the fact that 1,2-DO can assume a more compact packing arrangement in the interface than can 1,3-DO. The more compact packing of 1,2-DO is reflected in the vertical dotted lines in Figures 5 and 6 which show a concentration of 1,2-DO at the monolayer limit which is 20% higher than that of 1,3-DO. Additionally, the surface pressure–concentration isotherms for the lipids exhibit a similar relative difference at all surface pressures below collapse (not shown), and the collapse surface pressure for monolayers of 1,2-DO is 31.5 as compared to 27.7 mN/m for 1,3-DO (Table 1). The interaction of OOS with  $[^{14}\text{C}]$ colipase was unique in that the adsorption of  $[^{14}\text{C}]$ colipase was independent of OOS concentration in the interface. That does not imply a lack of interaction, however. Inspection of  $\pi_f$  values for  $[^{14}\text{C}]$ colipase adsorption to OOS (Figure 7) shows that  $\pi_f$  values considerably exceed the surface pressure accompanying  $[^{14}\text{C}]$ colipase adsorption in the absence of lipid and the collapse surface pressure of OOS, 13.2 mN/m. The reason for the unusual behavior of OOS in the context of all examined species is considered in detail below.

The procolipase activity-based assay used earlier to quantitate adsorbed procolipase gives considerably poorer

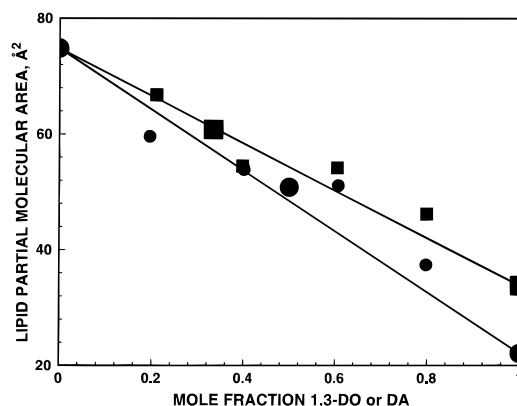


FIGURE 11: Dependence of lipid partial molecular area following [ $^{14}\text{C}$ ]colipase adsorption on monolayer lipid composition. SOPC was mixed with 1,3-DO (■) or DA (●). Larger symbols indicate values determined on the basis of at least 6 data points.

reproducibility than the radiometric procedure used to measure colipase adsorption in the present study. Inspection of Figures 3–6 and 8–10 in the entire range of  $\Gamma_L$  values below the monolayer limit shows that the values of  $\Gamma_C$  exhibit patterns of behavior which can be reasonably fit to a linear model from  $\Gamma_L = 0$  to the monolayer limit (not shown). However, with the better precision of the radiometric assay, it is clear that this model is an oversimplified description of the dependence of [ $^{14}\text{C}$ ]colipase adsorption on  $\Gamma_L$  and, presumably, the data for procolipase adsorption. As a consequence of these better data, the regions of differing adsorption behavior in Figures 3–6 and 8–10 must be considered as a function of  $\Gamma_L$  rather than in aggregate.

Linearity between  $\Gamma_C$  and  $\Gamma_L$  is observed over a range of  $\Gamma_L$  for SOPC, 1,2-DO, 1,3-DO, and DA (Figures 3–6 and 9–10, open squares), consistent with the simple geometric model proposed earlier (20). In this range of  $\Gamma_L$ , the intercepts on the ordinate and abscissa of lines fitted to this data (Figures 3–6 and 9–10, dashed lines) yield the reciprocals of the partial molar areas of the [ $^{14}\text{C}$ ]colipase and lipid, respectively (20). These are given in Table 1. For other lipid mixtures studied (e.g., Figure 8), estimates of partial molecular areas were made on the basis of 2 point lines. These are also given in Table 1 but were not used to compute averages. The partial molecular area of [ $^{14}\text{C}$ ]colipase calculated from the dashed lines obtained with the more extensive data sets shown in Figures 3–6 and 9–10 is  $498 \text{ Å}^2/\text{molecule}$ . The partial molar areas calculated for the pure lipids and mixtures, expressed per molecule, are also given in Table 1 and those for mixtures of SOPC with 1,3-DO and DA are shown in Figure 11 as a function of lipid composition. The larger symbols denote values for which more extensive data sets ( $>6$  points) were available to reasonably test the linear hypothesis. The apparent linearity shown in Figure 11 suggests that there is no unique interaction of the lipids in mixtures in the presence of [ $^{14}\text{C}$ ]colipase, *i.e.*, that when compressed by [ $^{14}\text{C}$ ]colipase to their apparent partial molecular areas of 75, 34, and  $22 \text{ Å}^2/\text{molecule}$  (Table 1), respectively, they mix ideally. An essential difference between the conclusions of this and the earlier study is that in the linear range, the values of the partial molecular areas of the substrates indicate that they are monomolecular, although highly compressed or condensed with colipase.

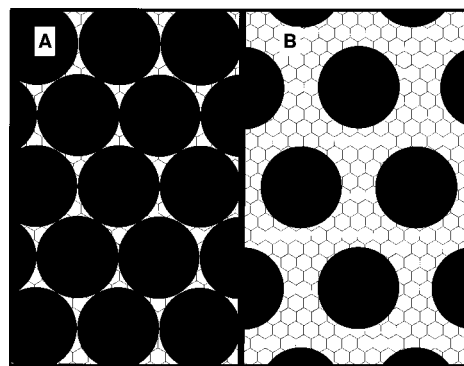


FIGURE 12: Packing of lipid acyl chains and colipase. Panels A and B depict the surface at the limits of linear behavior of  $\Gamma_C$  vs  $\Gamma_L$  as shown in Figures 2–5 and 8–9. The scale is based on colipase and lipid having a molecular area of  $500$  and  $20 \text{ Å}^2/\text{molecule}$ , respectively. Apparent molecular areas of colipase are  $550$  (A) and  $1100 \text{ Å}^2$  (B).

In examining the patterns of behavior for [ $^{14}\text{C}$ ]colipase adsorption to the various lipid monolayers shown in Figures 3–10, one feature is common to all lipids tested, including OOS. In the range of low  $\Gamma_L$ , specifically the range from 0 to  $\sim 3$  acyl chains per [ $^{14}\text{C}$ ]colipase adsorbed,  $\Gamma_C$  is nearly constant at  $28\text{--}30 \text{ pmol}/\text{cm}^2$ . Over this same range there is a large increase in  $\pi_f$  values accompanying the [ $^{14}\text{C}$ ]colipase adsorption. For the data in Figures 3–7 and 9–10, the values of  $\pi_f$  at a  $\Gamma_L$  of  $90 \text{ pmol}/\text{cm}^2$  of lipid chains, about 3 chains per [ $^{14}\text{C}$ ]colipase adsorbed, are between 21 and  $24 \text{ mN}/\text{m}$ . This means that the lipid acyl chains are stabilizing the interface without affecting [ $^{14}\text{C}$ ]colipase adsorption and without regard to lipid headgroup. Considering the size difference between the lipid molecules and [ $^{14}\text{C}$ ]colipase, this behavior suggests that the stabilization of the interface by small amounts of lipid while [ $^{14}\text{C}$ ]colipase adsorption is essentially constant arises from the filling of packing voids by lipid. Those voids would be essentially filled at 3 acyl chains per colipase molecule, *i.e.*, at approximately the left-hand limit of linear behavior shown in Figures 3–6 and 9–10, open squares. This is shown pictorially in Figure 12A which makes the assumption of circular cross sections for colipase and hexagonal packing of all molecules. The drawing is approximately to scale. Such a model is consistent with the average of  $33.4 \text{ pmol}/\text{cm}^2$  for the reciprocal of the partial molar area of [ $^{14}\text{C}$ ]colipase (Table 1) being 11% higher than the value of  $30.1 \pm 1.1 \text{ pmol}/\text{cm}^2$  observed for [ $^{14}\text{C}$ ]colipase in the absence of lipid. From geometric calculation, the area of a hexagon circumscribing a circle is 10.3% larger than the circle. It should be noted, however, that this agreement is only approximate because the shape of colipase in the plane of the interface is more rectangular than circular (26). The right-hand  $\Gamma_L$  limit of linear  $\Gamma_C$  vs  $\Gamma_L$  behavior for each lipid shown in Figures 3–6 and 9–10 occurs at  $18\text{--}25$  acyl chains per [ $^{14}\text{C}$ ]colipase molecule adsorbed. Again considering the size difference between the molecules, this stoichiometry suggests a packing arrangement as shown in Figure 12B. The figure shows that the end of the linear region corresponds to each pair of colipase molecules being separated by about 2 acyl chains. Although Figures 12A,B is an oversimplification, it shows approximately how much of the interface is occupied by lipid and protein at the beginning and end of the linear segments indicated in Figures 3–6 and 9–10.

That linearity ceases when [ $^{14}\text{C}$ ]colipase molecules are separated by approximately 2 acyl chains indicates that the stabilizing interactions, which are indicated by the increase in  $\pi_f$  values over the linear region (Figures 3–6), are relatively short range. Those interactions are negligible for SOPC for which  $\pi_f$  changes less than 2 mN/m between a  $\Gamma_L$  of 45 pmol/cm<sup>2</sup>, which is equivalent to  $\sim 3$  acyl chains per [ $^{14}\text{C}$ ]colipase, and the end of the linear region (Figure 3). However, fluorescence microscopy showed that, within the limits of resolution of the technique, SOPC and colipase are miscible. For the lipase substrates other than OOS, considered over the same range of 3 acyl chains per [ $^{14}\text{C}$ ]colipase to the end of the linear range, substantial increases in  $\pi_f$  are observed. For 1,3-DO, 1,2-DO, and DA, the values are approximately 10, 8, and 16 mN/m, respectively. Thus, the stabilization which occurs as lipid chains pack around [ $^{14}\text{C}$ ]colipase is lipid species specific and provides the molecular basis of the preferential interaction of [ $^{14}\text{C}$ ]colipase with some lipase substrates relative to SOPC. The absence of a linear range for [ $^{14}\text{C}$ ]colipase adsorption to OOS and the absence of substantial increases in  $\pi_f$  following a stoichiometry of 2–3 acyl chains/[ $^{14}\text{C}$ ]colipase suggest that this weakly surface-active lipid is simply excluded from the interface into a bulk lipid phase or an ordered lipid layer(s) above the monolayer. That the latter may occur is suggested by the behavior of  $\pi_f$  in the monolayer region (Figure 7) and the propensity of triacylglycerols to assume layered structures at interfaces (27, 28).

For SOPC, increasing  $\Gamma_L$  beyond the end of the linear range (Figure 3) leads to progressively lower adsorption of [ $^{14}\text{C}$ ]colipase with a gradual increase in  $\pi_f$ . This suggests that [ $^{14}\text{C}$ ]colipase with an annulus of lipid chains is miscible with SOPC in this range. For 1,3-DO and 1,2-DO, increasing  $\Gamma_L$  beyond the end of the linear range (Figures 5 and 6) induces no additional change in  $\Gamma_C$ , but  $\pi_f$  increases by 4–6 mN/m before becoming constant. This indicates the formation of a more tightly packed monolayer or, possibly, a multilayer structure in this range. Like triacylglycerols, diacylglycerols can also form layered structures (28, 29) by extending their acyl chains in opposite directions relative to the interfacial plane. The range of  $\Gamma_L$  in which both  $\Gamma_C$  and  $\pi_f$  are constant is presumably one in which the excess diacylglycerol is expelled into a bulk phase. Interestingly, increasing the surface concentration of DA beyond the linear range leads not only to an increase of 5 mN/m in  $\pi_f$  but also to a  $\sim 40\%$  increase in  $\Gamma_C$  as well. Consideration of the partial molecular areas of the components precludes this being the monolayer phase unless the [ $^{14}\text{C}$ ]colipase assumes a markedly smaller area in the interface. More likely is that some layering of the fatty acid (28, 30) or both components occurs. It is possible that [ $^{14}\text{C}$ ]colipase could be solubilizing DA from the interface into the aqueous phase in this range of  $\Gamma_L$  to achieve a more energetically favorable ratio of DA to [ $^{14}\text{C}$ ]colipase in the interface. Although we cannot exclude this possibility, it is inconsistent with the minimum in  $\Gamma_C$  observed at lower  $\Gamma_L$ . Were dissolution occurring in these adsorption experiments,  $\Gamma_C$  should have remained at a constant value above a  $\Gamma_L$  of 300 pmol/cm<sup>2</sup> (Figure 4). Additional studies will be required to determine if a novel structure is, indeed, formed when fatty acid is present in great excess and if this putative structure has consequences for the binding and adsorption of pancreatic lipase.

Based on the combination of surface pressure increases and measurements of [ $^{14}\text{C}$ ]colipase adsorption, the present study clearly shows specificity in the interaction of colipase with lipid species and their mixtures. Although the present study was conducted in the absence of bile salts, these are relatively weak surfactants. Unless bile salts interact specifically with colipase, our data support the suggestion (20) that colipase plays an additional role in lipolysis beyond helping pancreatic lipase to bind to the interface in the lid-open conformation. One possibility is that the relatively poor ability of colipase to adsorb to diacylphosphatidylcholine would minimize its adsorption to particles which are devoid of substrate. Likewise, when all substrate in a particle has been hydrolyzed and sufficient bile salts are present to remove fatty acids and monoacylglycerols, colipase may encourage the dissociation of the pancreatic lipase–colipase complex from the interface. Lastly, the relative affinities of colipase for triacylglycerols, diacylglycerols, and fatty acids will govern the concentrations of these species in its vicinity and, hence, that of pancreatic lipase. Thus, specificity in colipase–substrate interactions may regulate substrate availability to pancreatic lipase with respect to lipid species. An intriguing, but untested, possibility is that colipase–lipid interactions may also contribute to the acyl chain specificity of pancreatic lipase observed for substrates of the same type (31).

## ACKNOWLEDGMENT

We thank Dr. R. Pagano of the Mayo Medical School for the use of his epifluorescence microscopy equipment and Dr. R. E. Brown for his critical review of the manuscript.

## REFERENCES

1. Carriere, F., Barrowman, J. A., Verger, R., and Laugier, R. (1993) *Gastroenterology* 105, 876–888.
2. Carey, M. C., Small, D. M., and Bliss, C. M. (1983) *Annu. Rev. Physiol.* 45, 651–677.
3. Rudd, E. A., and Brockman, H. L. (1984) in *Lipases* (Borgström, B., and Brockman, H. L. Eds.) pp 185–204, Elsevier Science Publishers, Amsterdam.
4. Verger, R. (1984) in *Lipases* (Borgström, B., and Brockman, H. L., Eds.) pp 83–150, Elsevier Science Publishers, Amsterdam.
5. Lowe, M. E. (1994) *Gastroenterology* 107, 1524–1536.
6. Borgström, B., and Erlanson-Albertsson, C. (1984) in *Lipases* (Borgström, B., and Brockman, H. L., Eds.) pp 151–183, Elsevier Science Publishers, Amsterdam.
7. Erlanson-Albertsson, C. (1992) *Biochim. Biophys. Acta* 1125, 1–7.
8. Borgström, B., Wieloch, T., and Erlanson-Albertsson, C. (1979) *FEBS Lett.* 108, 407–410.
9. Larsson, A., and Erlanson-Albertsson, C. (1981) *Biochim. Biophys. Acta* 664, 538–548.
10. Egloff, M.-P., Sarda, L., Verger, R., Cambillau, C., and van Tilbeurgh, H. (1995) *Protein Sci.* 4, 44–57.
11. Wieloch, T., Borgström, B., Pieroni, G., Pattus, F., and Verger, R. (1981) *FEBS Lett.* 128, 217–220.
12. Erlanson-Albertsson, C., Weström, B., Pierzynowski, S., Karlsson, S., and Ahrén, B. (1991) *Pancreas* 6, 619–624.
13. Erlanson-Albertsson, C. (1992) *Nutr. Rev.* 50, 307–310.
14. Larsson, A., and Erlanson-Albertsson, C. (1991) *Biochim. Biophys. Acta* 1083, 283–288.
15. Larsson, A., and Erlanson-Albertsson, C. (1986) *Biochim. Biophys. Acta* 876, 543–550.
16. Wieloch, T., Borgström, B., Pieroni, G., Pattus, F., and Verger, R. (1982) *J. Biol. Chem.* 257, 11523–11528.



17. Gargouri, Y., Pieroni, G., Riviere, C., Lowe, P. A., Saunier, J.-F., Sarda, L., and Verger, R. (1986) *Biochim. Biophys. Acta* 879, 419–423.
18. Muderhwa, J. M., and Brockman, H. L. (1992) *J. Biol. Chem.* 267, 24184–24192.
19. Smaby, J. M., Muderhwa, J. M., and Brockman, H. L. (1994) *Biochemistry* 33, 1915–1922.
20. Momsen, W. E., Momsen, M. M., and Brockman, H. L. (1995) *Biochemistry* 34, 7271–7281.
21. Schmit, G. D., Momsen, M. M., Owen, W. G., Naylor, S., Tomlinson, A., Wu, G., Stark, R. E., and Brockman, H. L. (1996) *Biophys. J.* 71, 3421–3429.
22. Smaby, J. M., and Brockman, H. L. (1990) *Biophys. J.* 58, 195–204.
23. Momsen, W. E., & Brockman, H. L. (1997) *Methods Enzymol.* (in press).
24. Pagano, R. E., Martin, O. C., Kang, H. C., and Haugland, R. P. (1991) *J. Cell Biol.* 113, 1267–1279.
25. Hernell, O., Staggers, J. E., and Carey, M. C. (1990) *Biochemistry* 29, 2041–2056.
26. van Tilbeurgh, H., Sarda, L., Verger, R., and Cambillau, C. (1992) *Nature* 359, 159–162.
27. Bursh, T., Larsson, K., and Lundquist, M. (1968) *Chem. Phys. Lipids* 2, 102–113.
28. Larsson, K. (1973) *Surf. Colloid Sci.* 6, 261–285.
29. Dorset, D. L., and Pangborn, W. A. (1978) *Z. Naturforsch. C: Biochem. Biophys.* 33C, 39–49.
30. McFate, C., Ward, D., and Olmsted, J., III (1993) *Langmuir* 9, 1036–1039.
31. Chen, Q., Bläckberg, L., Nilsson, Å., Sternby, B., and Hernell, O. (1994) *Biochim. Biophys. Acta* 1210, 239–243.

BI9703857